

# Visible Light Photocatalytic Degradation of Methylene Blue and Malachite Green Dyes with BaWO<sub>4</sub>-Go Nano Composite

M. Sunitha<sup>1,2</sup>, R. Soma Sekhar<sup>3</sup>, B.Ravali<sup>4</sup>, Ch. Rama Krishna Reddy<sup>1</sup>, S.V. Mahalakshmi<sup>1</sup>, V.Sruthi<sup>1</sup>, S. Paul Douglas<sup>1\*</sup>

<sup>1</sup>Department of Engineering Chemistry, AU College of Engineering (A), Andhra University, Visakhapatnam-530 003, (AP) India.

<sup>2</sup>SKR College for Women, Rajamahendravaram-533 103, (AP) India.

<sup>3</sup>ANITS College of Engineering, Sangivalasa, Visakhapatnam-531162.

<sup>4</sup>Centre for Nanotechnology, AU College of Engineering (A), Visakhapatnam-530 003, (AP) India

**Abstract**— A facile solid state metathesis synthesis of barium tungstate (BaWO<sub>4</sub>) followed by ball milling and subsequent preparation of barium tungstate-graphene oxide (BaWO<sub>4</sub>-GO) nano composite using a colloidal blending process and its application as a visible light photocatalyst for the degradation of Malachite green and Methylene blue dyes. The morphology and composition of barium tungstate (BaWO<sub>4</sub>) nano composite have been characterized using X-Ray Diffraction (XRD), UV-Visible Diffuse Reflectance Spectra (UV-DRS), Raman Spectra, Field Emission Scanning Electron Microscopy (FESEM) – EDAX and UV Visible Spectroscopy. This composite material is found to be a wide band gap semiconductor with band gap of 4.3 eV. The sample shows poor transmittance in ultraviolet region while it has maximum transmittance in visible-near infrared regions. It shows an increase in range and intensity of light absorption and the reduction of electron-hole pair recombination in BaWO<sub>4</sub> with the introducing of GO on to it.

**Keywords**— Barium Tungstate, Graphene Oxide, Metathesis, Photocatalytic Degradation, Methylene blue, Malachite green.

## I. INTRODUCTION

Waste water in textile industry is a major source of environmental pollution, since the remnant constituent dyes in the exhaust are non-biodegradable, highly toxic and impart persistent color of high intensity. Several methods have been proposed to decolorize such exhausts and to remove the organic pollutants by way of adsorption, bio-degradation, ozonation, chlorination etc. [1]. Recently, heterogeneous photo catalysis has emerged as an alternate method for decontamination of such organic pollutants, in which metal tungstate semiconductors are widely used as photo catalysts. Of the various metal tungstate, graphene oxide based metal

tungstates has been widely studied because of its high catalytic activity, high chemical stability and low cost. Hybrids materials, i.e., composites consisting of different materials, have emerged in materials science. Strong interactions at the interface between two different layers in a hybrid material can produce unexpected novel properties and can have synergetic effects [2], therefore they can be regarded as new materials due to the emergence of these new properties. Many hybrid materials have been studied such as metal-metal hybrids, metal-organic hybrids [3], inorganic semiconductors [4], inorganic-organic hybrids [5] and carbon materials [6]. The synthesis of hybrid materials has been demonstrated using several methods, including chemical vapor deposition (CVD) [7], template-assisted synthesis [8] and self-assembly methods [9]. These hybrid materials have Wolframite and Scheelite type structures which is commonly found in divalent metal ion tungsten type of crystals (AWO<sub>4</sub> or ABO<sub>4</sub> (A = Ba, Sr, Ca, Pb)). The Wolframite structure is made up of hexagonally closely packed oxygens with certain octahedral sites filled by A and B cations in an ordered way. These oxygens are not closely packed in the Scheelite structure and the coordination number of the A cation is eight while the B cation is in approximate five tetrahedral co-ordination to oxygen, which can be regarded as cubic close-packed array of A<sup>2+</sup> and BO<sub>4</sub><sup>2-</sup> units which are orderly arranged. The oxygens are three coordinated to cations in both the Scheelite and Wolframite structure. However, in Scheelite each oxygen is bound to two A cations and one B cation, where as in the Wolframite structure half are coordinated to two B cations and half are coordinated to two A cations, due to its divalent nature mostly in tungstates they have immense interest because of their remarkable properties such as luminescence, non-linear optical activity, photocatalysis, and scintillation [10–16]. Barium

tungstate ( $\text{BaWO}_4$ ) is the heaviest member of the family of the alkaline earth tungstates. Like many other  $\text{ABX}_4$  type compounds,  $\text{BaWO}_4$  crystallizes at ambient conditions in the tetragonal Scheelite-type structure (space group [SG]:  $I4_1/a$ , No. 88,  $Z = 4$ ) [17]. GO behaves strongly hydrophilic, and is easily exfoliated in water forming stable colloidal dispersions. The as-synthesized, graphite oxide typically possesses a carbon-to-oxygen ratio of about two, and the material is non-conducting. Each fundamental layer of GO consists of a dense two-dimensional carbonaceous skeleton containing a larger number of  $\text{sp}^3$  hybridized carbon atoms and a smaller number of  $\text{sp}^2$  carbons. It can be reduced either by heating or by external reducing agent, to form graphite like structure with turbostratic tendency containing few oxygen groups [18]. GO nanocomposites were regarded as novel photocatalyst for degradation of pollutants due to excellent electron conductivity and high transparency of graphene oxide. However, a slow electron transfer greatly limited to the extended applications in photocatalysis. It is introduced to improve the effective electron transfer of  $\text{BaWO}_4$  [19]. The addition of small concentrations of hydrogen peroxide ( $\text{H}_2\text{O}_2$ ) to photocatalytic systems may enhance the process efficiency. At higher concentrations, hydrogen peroxide was found to have an inhibiting effect on photo catalytic reactions [20]. Hydrogen peroxide can accelerate the reaction rate by capturing electrons, reacting with excess oxygen, or absorbing light with wavelengths shorter than 310 nm. In all situations described,  $\cdot\text{OH}$  radicals, which are critical during the process due to their high reactivity, are generated [21]. In this study, we have reported the synthesis of  $\text{BaWO}_4$  and  $\text{BaWO}_4$ -graphene oxide composites by adding small concentrations of  $\text{H}_2\text{O}_2$  to enhance the photocatalytic activity. The morphology and composition have been characterized using XRD, FT-IR, Raman spectra, SEM and EDAX.

## II. EXPERIMENT

### 1. Material and Methods

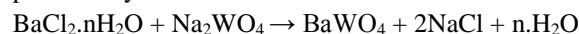
All the chemicals were purchased of analytical grade which can be used directly without any further purification. All the reactions were carried out using deionized water. The dyes used for this study are Malachite green and Methylene blue whose chemical formulae are  $\text{C}_{23}\text{H}_{25}\text{ClN}_2$  and  $\text{C}_{16}\text{H}_{18}\text{ClN}_3\text{S}$  respectively, and the stock solutions of the dyes were prepared in 10 ppm concentrations in distilled water.

### 2. General Procedure

#### 2.1 Synthesis of $\text{BaWO}_4$

$\text{BaWO}_4$  is prepared by solid-state metathesis synthesis followed by Ball milling. Stoichiometric amounts of  $\text{BaCl}_2$  (Loba Chemie Pvt. Ltd) and  $\text{Na}_2\text{WO}_4$  (98%

HIMEDIA) in the molar ratio of 1:1 are mixed in an agate mortar and ground for 4 hrs in ethanol. After 4hrs of grinding, at room temperature the compound is washed several times with distilled water to remove the by-product  $\text{NaCl}$  and then the residue is dried at  $80^\circ\text{C}$  in hot air oven. At the end of this process barium tungstate powder is obtained which is subjected to phase identification, micro structural investigation and photocatalytic studies.



The resultant compound  $\text{BaWO}_4$  obtained from the solid-state method was taken and ground mechanically in low energy ball mill to obtain nano sized metal tungstate. The balls to powder weight ratio is 10:1, the mixture is grinded at 350 rpm for 4 hrs in wet medium i.e. methanol to obtain homogeneous compound. The residue after ball milling was dried using hot air oven.

#### 2.2 Synthesis of Graphene oxide

Graphene Oxide (GO) was prepared by the well-known modified Hummers method [23] from an expanded acid washed graphite flakes. In this, 5 g of graphite was added into a mixture of 108 mL of  $\text{H}_2\text{SO}_4$  and 12 mL of  $\text{H}_3\text{PO}_3$  and stirred for 10 min. To it, 2.5 g of sodium nitrate was added. Subsequently, the beaker with reagents is kept in an ice bath to maintain the temperature at  $5^\circ\text{C}$ . Now, 15 g of  $\text{KMnO}_4$  was added in portions into the mixture, which was vigorously stirred. After addition of the oxidant, the beaker was heated and kept at  $35 - 40^\circ\text{C}$  with continuous stirring. In the next step, 280mL of deionized water was added to the beaker and heated to  $95^\circ\text{C}$  and maintained the same conditions for about 60 min. To complete the reaction 5 ml of 30%  $\text{H}_2\text{O}_2$  is added and the color of the solution gradually changes to bright yellow. The mixture is then washed with 5%  $\text{HCl}$  solution to remove sulfate ions and with deionized water to remove the chloride ions to maintain neutral pH. After centrifugation the gel like substance is vacuum dried at  $60^\circ\text{C}$  for more than 6 hrs to get GO as powder.

#### 2.3 Synthesis of $\text{BaWO}_4/\text{GO}$ Nano composites

$\text{BaWO}_4$  which is synthesized by Solid State Metathesis and GO which is synthesized by modified Hummers method are taken [23]. To prepare these nano composites, 1ml of 10% GO was dispersed in ethylene glycol solution under sonicator for 30 minutes and 1gm of barium tungstate is dispersed in GO solution. The above mixture is kept under continuous stirring for about 2 hours. A blackish coloured precipitate is collected washed with 10% ethanol and dried in vacuum oven at  $80^\circ\text{C}$  for 12 hours [24]. The obtained  $\text{BaWO}_4$ -GO composite was characterized by X-Ray Diffraction (XRD), FT-IR, Scanning Electron Microscopy (SEM) and EDS, UV-Diffused Reflectance Spectroscopy, Raman Spectroscopy.

### 3. Photo Catalytic Experiments

Photo catalytic activity of the synthesized BaWO<sub>4</sub>-GO nano composite was evaluated by de-colorization of Methylene blue and Malachite green dye solutions. The experiments were carried out under the visible light irradiation in presence of BaWO<sub>4</sub>-GO as photo catalyst. The photo catalysis process is carried out in a visible light photo reactor constructed with an outer wooden cabinet equipped with a magnetic stirrer, a 400 watt metal halide lamp, an exhaust fan and an electric power supply cable. The reaction was carried out by adding 0.05 gms of the as-synthesized nano composite and 2.5mL of H<sub>2</sub>O<sub>2</sub> into 1000 mL Borosil glass beaker containing 100 mL of dye solution (10 ppm). The suspension was magnetically stirred in dark for 30 minutes to obtain desorption/absorption equilibrium before irradiating the solution to the light. The solution was irradiated under halide lamp and aliquots were drawn at regular time intervals, centrifuged and the transparent dye solution analyzed for absorbance using visible spectrophotometer (Model No SYSTRONICS-105 with 340 nm to 960 nm).

Percentage degradation of the dye was calculated using the following formula.

$$\% \text{ Degradation} = \frac{A_0 - A_t}{A_0} \quad \text{equation (1)}$$

Where A<sub>0</sub> is absorbance of dye at initial stage A<sub>t</sub> is absorbance of dye at time t.

### 4. Instrumentation

Retsch® Planetary Ball Mill PM 100 bench top grinding station has been used for ball milling. The resulting powder was characterized using X-Ray Diffractometer (PANalytical- X' Pert PRO, Japan) at room temperature, using Nickel Filter Cu-K $\alpha$  radiation ( $\lambda = 1.54059 \text{ \AA}$ ), over a wide range of  $10^\circ \leq 2\theta \leq 80^\circ$  with a scanning speed of  $2^\circ \text{ min}^{-1}$ . The morphology of the as-synthesized samples was investigated by field emission scanning electron microscopy (FESEM, LEO1550). Band gaps were calculated using Single Monochromator UV-2600 (optional ISR-2600Plus,  $\lambda$  up to 1400nm). FT-IR spectral data were recorded from BRUKER ALPHA FT-IR with Opus 6.1 version and on a Perkin Elmer Spectra-880 spectrophotometer, using KBr pellets at 400-4500 cm<sup>-1</sup> region.

## III. RESULTS AND DISCUSSION

### 5.1 X-Ray Diffraction

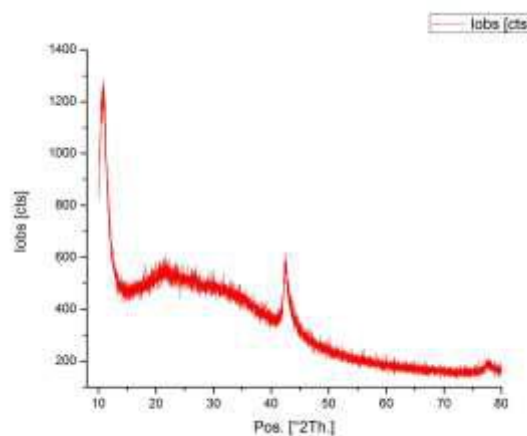


Fig.1: XRD-Spectrum of Graphene Oxide

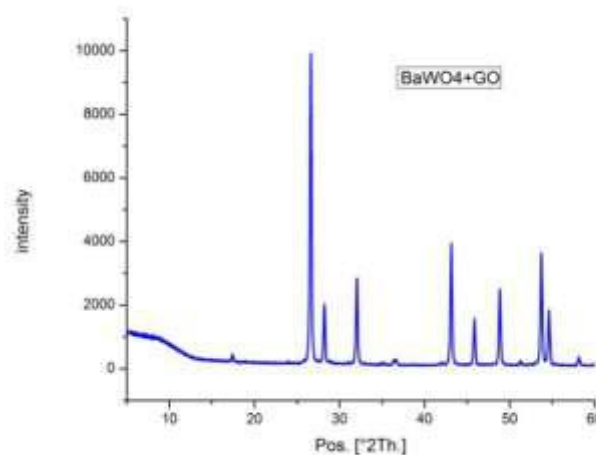


Fig.2: XRD pattern of Barium tungstate-GO composite

Fig-1 shows the X-Ray Diffraction plot of nano graphene oxide and Fig-2 shows the X-Ray Diffraction plot of BaWO<sub>4</sub>-GO nano composite. These peaks are in good agreement with the characteristic peaks of BaWO<sub>4</sub>. While a distinct peak for pure graphene oxide was observed at  $2\theta = 10.2^\circ$  (Fig-1). This GO related peak is not observed in BaWO<sub>4</sub>-GO plot due to the low amounts of GO and the resultant low diffraction intensity that would be below the limit of detection of the instrument [25]. The phase purity of the as-synthesized materials was confirmed by representative XRD analysis. As shown in Fig-2 the as-prepared powder samples have similar narrow characteristic peaks locating at  $17.1^\circ$ ,  $26.2^\circ$ ,  $28.8^\circ$ ,  $34.1^\circ$ ,  $43.2^\circ$ ,  $46.2^\circ$ ,  $47.2^\circ$  and  $49.4^\circ$ . These results suggested that all the diffraction peaks could be assigned to the tetragonal Scheelite phase where as  $a = 0.561 \text{ nm}$ ,  $c = 1.271 \text{ nm}$  of BaWO<sub>4</sub> with space group I41/a JCPDS card no. 85-0588 [26, 27].

### 5.2 Fourier Transform Infrared Spectroscopy

Optical studies of barium tungstate nano crystals FT-IR spectrum, shows a strong band at  $833\text{cm}^{-1}$  characteristic of W-O vibrations of the  $\text{WO}_4^{2-}$  group [28, 29] is shown in Fig-3. FTIR spectrum of  $\text{BaWO}_4$  nano crystals synthesized in aqueous medium have broad band at  $3448.75\text{ cm}^{-1}$  and at  $1632.52\text{ cm}^{-1}$  are due to the vibrations of adsorbed water molecules on the sample. The broadness is attributed to the characteristic nano nature of the particles [30].

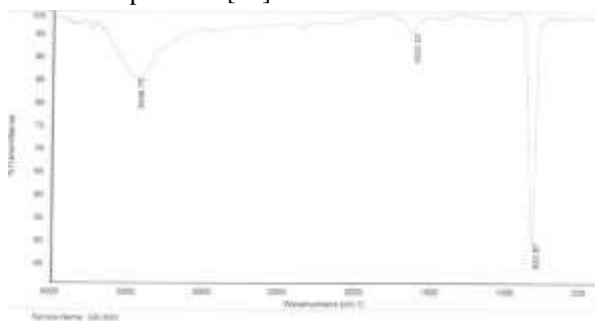


Fig.3: FT-IR spectra of barium tungstate and Graphene Oxide composite

### 5.3 Composition and Morphology Study

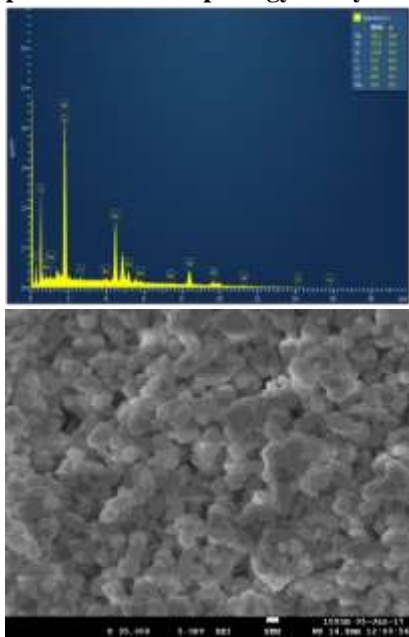


Fig.4: SEM images and EDS of barium tungstate and graphene Oxide composite

The nano structures and morphologies of samples are examined by SEM characterization. It shows that the nano structured  $\text{BaWO}_4$  particles have a rough surface, than the  $\text{BaWO}_4$ -GO nano composites, due to its irregular particles anchored on the surface of  $\text{BaWO}_4$ . From this, it can be clearly observed that the prepared sample consists of nano particles in the size of  $<50\text{ nm}$  in diameter. The well defined particle features of the tungstates synthesized by SSM reactions showed that these reactions have control

over morphology of the final products samples is confirmed by EDAX analysis. The atomic percentages of each element are Ba-39%, W-37.8%, O-12.6% and C-6.3%. These results show that appropriate quantities of Ba, W and O are present in the samples which is shown in Fig. 4. Among Scheelite tungstates, SEM showed granule-like features for Ba materials. When the net inorganic surface charge was negative ( $[\text{Ba}^{2+}]/[\text{WO}_4^{2-}] < 1$ ), the initially formed particles of  $\text{BaWO}_4$  had a negative charge due to the excess  $\text{WO}_4^{2-}$  ions. These particles are strongly interacted with cationic surfactants and played an important role in the morphology of  $\text{BaWO}_4$  products [31].

### 5.4 UV Diffuse Reflectance Spectral Studies

The optical properties of pure  $\text{BaWO}_4$ , nano  $\text{BaWO}_4$  and  $\text{BaWO}_4$ -GO composite were evaluated by UV-diffuse reflectance spectroscopy, shown in Fig 5. The optical absorbance spectra for  $\text{BaWO}_4$  nanoparticles and  $\text{BaWO}_4$ -GO appeared in the ultraviolet region 285nm, by introducing graphene oxide on the surface of nano  $\text{BaWO}_4$ , there was a similar absorption edge with nano  $\text{BaWO}_4$ , indicating that the graphene oxide was not incorporated into the lattice of  $\text{BaWO}_4$  and just got adsorbed on its surface [32].

It was reported that absorption is a powerful, non-destructive technique to explore the optical properties of sample. To calculate the direct band gap of the sample, UV-DRS uses Tauc relationship is

$$\alpha h\nu = A(h\nu - E_g)^n \quad (2)$$

Where, ' $\alpha$ ' is the absorption coefficient, 'A' is a constant and  $n = 1/2$  for direct band gap sample.

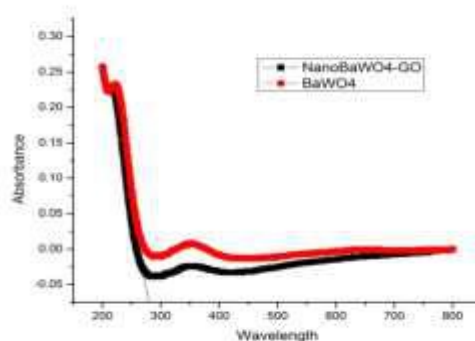


Fig.5(a): Band gap spectrum of  $\text{BaWO}_4$  and nano  $\text{BaWO}_4$

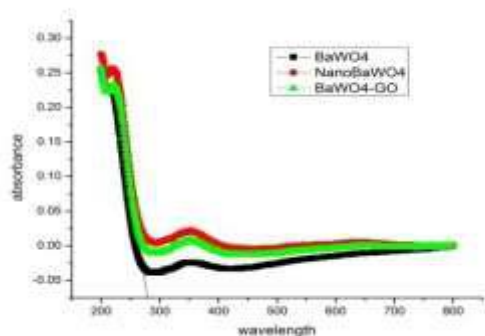


Fig.5(b): nano BaWO<sub>4</sub> and nano BaWO<sub>4</sub>- GO composite  
 From the plot of absorbance Vs wavelength ( $\lambda$ ), wavelength of the material is estimated and band gap is calculated from the equation

$$E_g = \frac{1240}{\lambda(\text{nm})} \quad \text{equation (3)}$$

Where  $\lambda$  is the Wavelength of the material from the graph.  $E_g$  is the bandwidth to be calculated. As show in Fig 5.a and Fig 5.b, the optical absorbance spectra for BaWO<sub>4</sub>, nano BaWO<sub>4</sub> and nano BaWO<sub>4</sub>-GO nano composite appeared as 285 nm. The measured optical band gap ( $E_g$ ) for BaWO<sub>4</sub> is 4.3 eV [33].

The basic optical properties and optical constants of the nano BaWO<sub>4</sub> are studied using UV-visible absorption spectroscopy which showed that the material has a wide band gap semiconductor with band gap of 4.3 eV. The sample shows poor transmittance in ultraviolet region while maximum in visible-near infrared regions.

As the band gap is the energy difference between valance and conduction band, the presence of these intermediate levels resulted in the reduction of optical band gap energy. The BaWO<sub>4</sub> prepared by the present method possess wide band gap along with good transmittance in the visible region which is suitable for transparent conducting oxide films of window layers on solar cells [31].

### 5.5 Raman Spectral Analysis

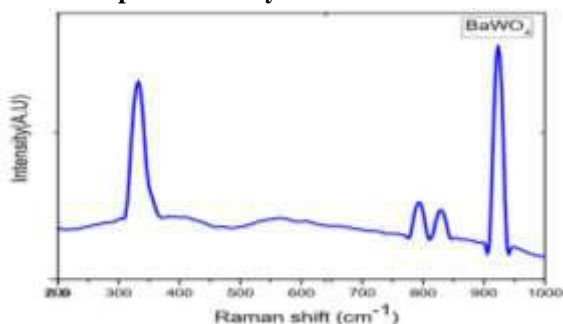


Fig.6: Raman spectra of BaWO<sub>4</sub>-GO nano composite

The Raman spectra of Scheelite crystals can be divided into two groups, internal and external. The first is called lattice phonon mode which corresponds to the motion of Ba<sup>2+</sup> cation and the rigid molecular unit. The second belongs to the vibration of inside [WO<sub>4</sub>]<sup>2-</sup> molecular units

with the centers of mass stationary. Raman-active phonon modes can be employed to estimate the structural order at a short range of a material. We expect 13 Raman-active modes in BaWO<sub>4</sub>. All the observed Raman modes are the characteristics of a Scheelite tetragonal [9, 40–42]. The internal modes] 1(*A<sub>g</sub>*), ]2(*E<sub>g</sub>*), ]3(*E<sub>g</sub>*), and ]4(*B<sub>g</sub>*) were observed at 924, 842, 790 and 345cm<sup>-1</sup> [30] shown in Fig.6.

### 5.6 UV-Visible spectroscopy

The UV-Vis spectral range is approximately at 200 to 800 nm, as defined by the working range of typical commercial UV-Vis spectrophotometers. The short-wavelength limit for simple UV-Vis spectrometers has the absorption of ultraviolet wavelengths less than 180 nm by atmospheric gases. Purging a spectrometer with nitrogen gas extends this limit to 175 nm. Working beyond 175 nm requires a vacuum spectrometer and a suitable UV light source.

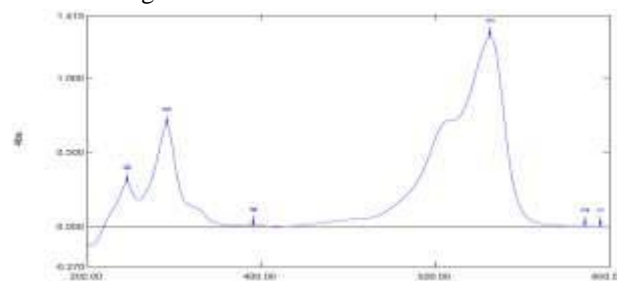


Fig.7: Methylene blue UV-Visible spectra

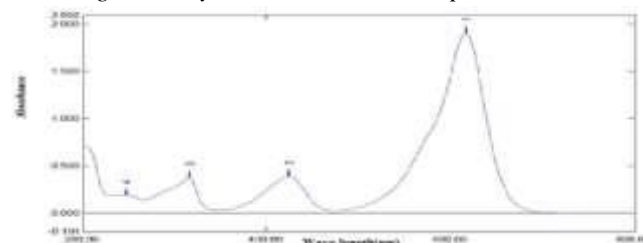


Fig.8: Malachite green UV- Visible Spectra

Fig. 7&8 shows that high intensity peak at 667nm for Methylene blue and 617 nm for Malachite green respectively. The absorption wavelength of Methylene blue was maintained at 667 nm and Malachite green was maintained at 617 nm throughout the study and the percentage of degradation of Methylene blue, Malachite green was carefully monitored at various time intervals.

### 5.7 Photo Catalytic Activity Studies

The photo catalytic activity of the nano BaWO<sub>4</sub>-GO composite was investigated towards the degradation of organic dyes Methylene blue (MB) and Malachite green under visible light irradiation is represented in Fig. 9 which shows the comparison between micro, nano BaWO<sub>4</sub> and BaWO<sub>4</sub>-GO nano composite. Aiming at eliminating the effect of adsorption on the dye degradation efficiency, before each photocatalytic process, the adsorption-desorption equilibria between the

dye and the photocatalysts were first obtained at 30 min and it is sufficient time to reach equilibrium. After 30 min the reaction mixture is exposed to visible light under constant magnetic stirring and aliquot of the reaction mixture is collected for every 10 min and subjected to UV-Vis analysis. It can be seen that the intensity of the absorption peaks decreased as the reaction progressed with BaWO<sub>4</sub>-GO as the catalyst. For getting 100% degradation MG takes 110 min and for MB takes 90 min shown in Fig. 9a and 9b.

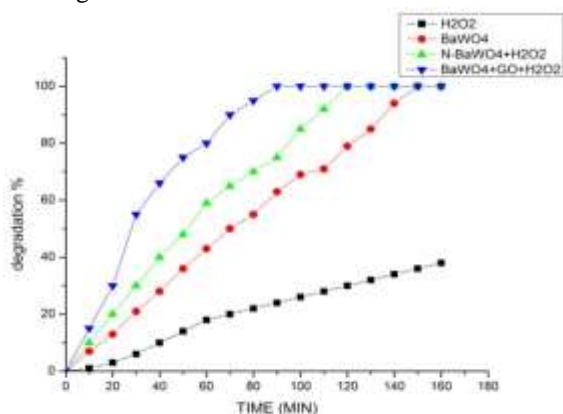


Fig.9a: MB degradation curves

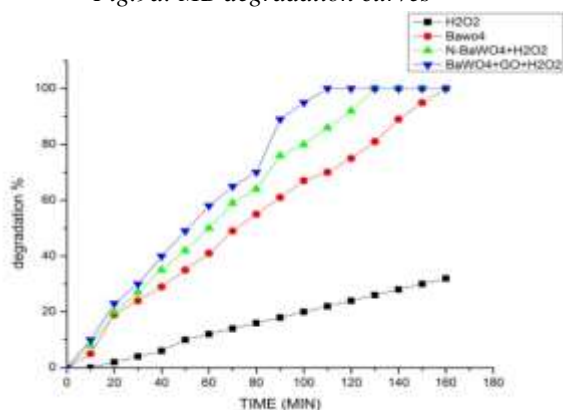


Fig.9b: MG degradation curves

Fig - 9a&9b Photo degradation plots of Malachite green and Methylene blue with barium tungstate, nano barium tungstate and barium tungstate –graphene oxide nano composite.

### 5.8 Effect of Graphene oxide % composition on the photocatalytic activity

Malachite green and Methylene blue dye can be more easily adsorbed by GO (MG&MB degradation efficiency ~75%) rather than the BaWO<sub>4</sub> (MG&MB degradation efficiency ~3%) catalyst. Its adsorption capacity was enhanced when GO was introduced on BaWO<sub>4</sub>. The performances of the prepared samples, including pure BaWO<sub>4</sub> and modified BaWO<sub>4</sub> by graphene oxide with different percent compositions were investigated with regard to the degradation of MG&MB under visible light irradiation. There is almost no photodegradation in the

absence of the catalyst. This suggested that, negligible amount of degradation by light can be ignored. In the presence of nano BaWO<sub>4</sub>, for Malachite green and Methylene blue dyes 110 to 120 min is sufficient to degrade under visible light irradiation. The BaWO<sub>4</sub>-GO nano composite has enhanced the photocatalytic degradation of Malachite green and Methylene blue dyes. The efficiencies of dye degradation were significantly improved from 80% to 100% in a time interval of 60 to 80 min by improving the amount of graphene oxide from 5% to 10% in the BaWO<sub>4</sub>-GO composite. Even though by adding up to 20% of graphene oxide in the composite, degradation efficiency remained the same shown in Fig. 10 and Table 1. This suggests that graphene oxide with an amount of 10% in the BaWO<sub>4</sub>-GO composite performs the best in removing the organic pollutants in waste water under visible light irradiation.

Table.1: Effect of loading of GO on catalyst

Entry	Catalyst loading	Degradation %
1	Blank	0
2	10mg	45
3	20mg	80
4	50mg	100
5	100mg	100
6	200mg	95
7	500mg	87
8	1000mg	75

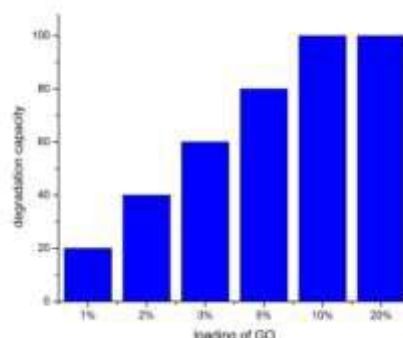


Fig.10: % of GO Composition on catalyst

### 5.9 Effect of Photo catalysts Dosage

A number of reports have demonstrated that catalyst dosage has a large influence on the reaction rate. The effect of photocatalysts (10% BaWO<sub>4</sub>-GO nano composite) dosage on the photocatalytic degradation of Malachite green and Methylene blue was studied and shown in Fig. 11. The dosage amount was varied from 10mg to 100mg/100ml and all the observations are carried out at room temperature. It can be concluded that, with the increase in amount of catalyst dosage from 10mg to 50mg/100ml, the degradation efficiencies were significantly improved. This phenomenon is may be due

to increase in the amount of catalysts dosage, which would increase the reactive sites that can correspondingly produce more reactive oxidative species. However, too much catalyst dispersed in the system will possibly increase light scattering and decrease light penetration [28], resulting in the reduction of degradation efficiency of MG&MB in a system with excessive photocatalysts. 10% and 20% GO-nano BaWO<sub>4</sub> are having similar percentage of degradation composite performs the best in removing the organic pollutants in wastewater under visible light irradiation, shown in Table 2. So the experiment was carried out with 10%GO-Nano composite.

Table.2: Effect of Loading of BaWO<sub>4</sub>-GO Catalyst

Entry	Catalyst loading	Degradation %
1	Blank	0
2	10mg	45
3	20mg	80
4	50mg	99
5	100mg	99
6	200mg	95
7	500mg	87
8	1000mg	75

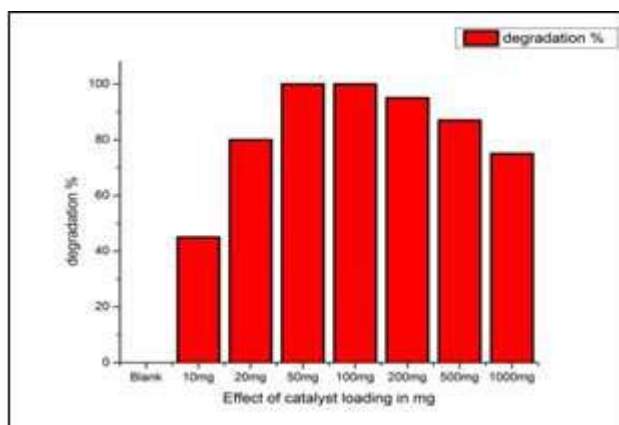


Fig.11: Effect of photo catalytic dosage on MB and MG

### 5.10. Effect of amount of H<sub>2</sub>O<sub>2</sub>

The effect of the initial H<sub>2</sub>O<sub>2</sub> dosage on the decomposition efficiency of dye (MB/MG), shown in Fig.12. The oxidation degradation conversion of dye(MB/MG) increased and reached a maximum when the amount of H<sub>2</sub>O<sub>2</sub> added was 2.5mL. After that, the decolourization efficiency drastically decreased as the amount of H<sub>2</sub>O<sub>2</sub> was further increased. When the amount of H<sub>2</sub>O<sub>2</sub> was first increased, more reactive radicals were generated on the surface of BaWO<sub>4</sub>-GO composite. At lower concentration, H<sub>2</sub>O<sub>2</sub> inhibits the recombination of photogene rated electrons and holes and higher concentration, H<sub>2</sub>O<sub>2</sub> is a powerful OH· scavenger, which would decrease the oxidation activity, is shown in Table 3. Therefore it is necessary to choose a proper amount of H<sub>2</sub>O<sub>2</sub> according to the kinds and concentrations of

pollutants in order to optimize the oxidation efficiency of H<sub>2</sub>O<sub>2</sub> [34].

Table.3: Effect of loading of H<sub>2</sub>O<sub>2</sub>

Loading of H <sub>2</sub> O <sub>2</sub>	% Degradation of dye
1	86
1.5	91
2	98
2.5	98
3	85
3.5	80

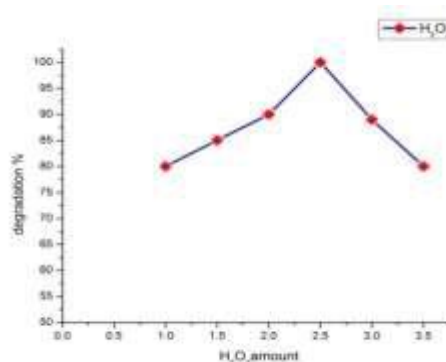


Fig.12: Effect of amount of H<sub>2</sub>O<sub>2</sub>

### 5.11 Effect of pH of Initial dye Solution

Considering that the pH of waste water is possibly different, its effect on the photocatalytic degrading dye (MG/MB) in the presence of BaWO<sub>4</sub>-GO under visible light irradiation was explored. It has been reported that, with an increase of pH of the dye (MG/MB) solution, it may reduce the adsorption of dye (MG/MB) on the photocatalyst. This resulted in the improvement of degradation efficiencies when pH of the MG solution increased to 8 and for MB solution increased from 8 to 9 [35] is shown in Table.4 and Fig. 3. The transformation of BaWO<sub>4</sub> damages the BaWO<sub>4</sub>-GO structure and eventually reduces the photocatalytic activity.

Table.4: Effect of pH Vs % degradation of MG and MB

pH	% Degradation of MG	% Degradation of MB
6	90	90
7	94	95
8	98	198
9	95	98
10	89	90

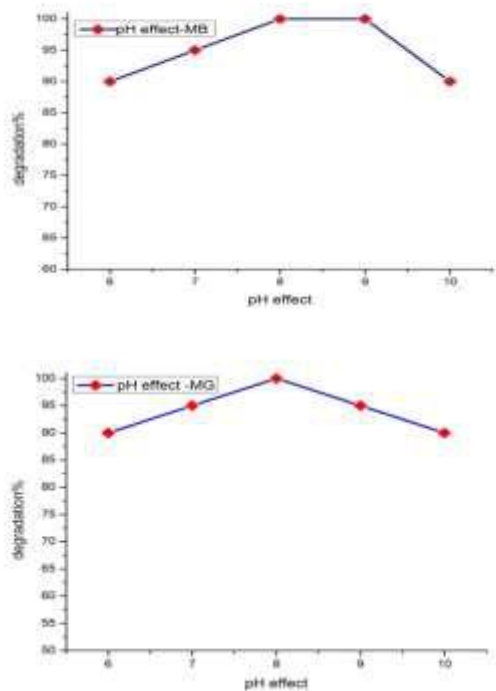


Fig.13: pH range of BaWO<sub>4</sub>-GO nano composite on Malachite green and Methylene blue

### 5.12 Effect of Temperature

Temperature of the photocatalytic reacting system was also varied from 0 to 80°C to explore its effect on the photocatalytic performances of the prepared samples under visible light irradiation. When the temperature of the reacting system is in the range of 20–60°C, the photocatalytic performances in degrading dye (MG/MB) were similar, and only slight increases were found with the increase in temperature shown in Fig.14. However when the temperature was fixed at 0°C, the photocatalytic activity was significantly reduced, this might be due to the decreased mass transfer of pollutants to the surface of photocatalysts and the decreased generation rate of oxidative species. When the temperature was as high as 80°C, the photocatalytic activity was greatly decreased. High temperature favors the recombination of charge carriers and desorption of adsorbed organics on the photocatalysts. These results can be regarded as evidence of temperature controller needed for solar devices.

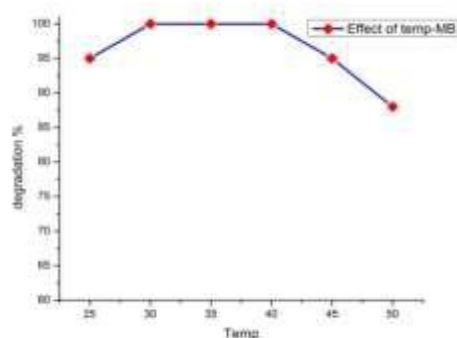
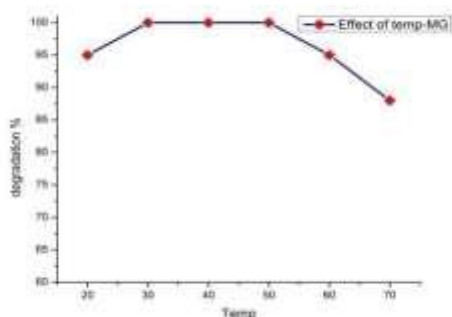


Fig.14: Effect of temperature of MB and MG

### 5.13 Reusability of the catalyst

Reusability of the catalyst (BaWO<sub>4</sub>-GO composite) was also studied under the optimized conditions. After the reaction finished, the catalyst was recovered and washed with distilled water and ethyl alcohol. The recovered catalyst was treated again by H<sub>2</sub>O<sub>2</sub> for the next degradation run. The removal efficiency of dye (MG/MB) was 90% in the first run, 60% in second run and 25% in the third run over 80-150 min under visible light irradiation shown in Fig-15 and table 5&6 . The slight decrease can be attributed to the loss of photocatalysts between two runs and some refractory intermediates adsorbed on their surface which are difficult to be destroyed [36]. Despite this slight reduction in removal efficiency, the stability of the reused BaWO<sub>4</sub>-GO photocatalysts after degradation of dye (MG/MB) is still significant.

Table.5: Reusable capacity of catalyst in MG

No of runs	recoverability %
First run	90
Second run	60
Third run	28

Table.6: Reusable capacity of catalyst in MB

No of runs	Recoverability %
First run	90
Second run	58
Third run	25

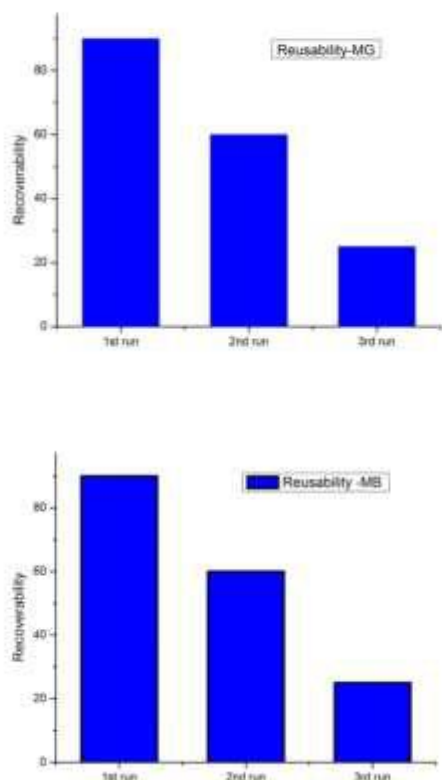
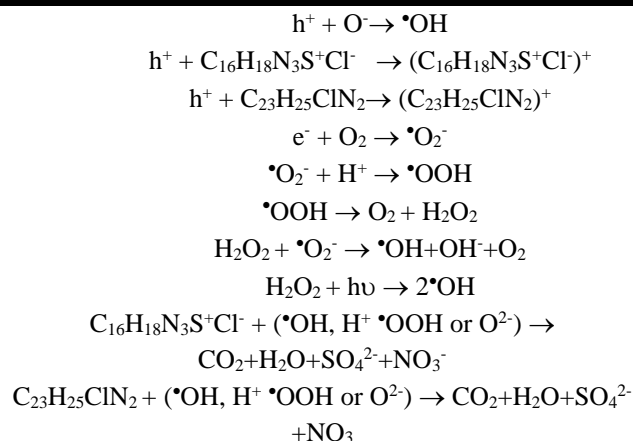
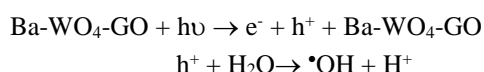


Fig.15: Reusable capacity of MG and MB on BaWO<sub>4</sub>-GO nano composite

### 6. Plausible Photocatalytic Mechanism

The plausible mechanism for the photocatalytic activity of the catalyst can be attributed to the presence of  $\pi$ -conjugation and 2D planar structures of graphene oxide in the BaWO<sub>4</sub>-GO composite which can adsorb organic molecules easily on its surface via strong  $\pi$ - $\pi$  interactions [30]. Additionally, graphene oxide possesses high charge carrier mobility and can be regarded as an electron acceptor. It can greatly decrease the recombination rate of photo-generated electrons and holes. Upon visible light excitation, the electron-hole pairs ( $h^+$ ,  $e^-$ ) are generated on the Barium tungstate-graphene oxide surface followed by the instant transfer of photo-generated electrons onto graphene oxide via a percolation mechanism and then the negatively charged graphene oxide can activate the dissolved oxygen to produce superoxide anion radical, while the holes can react with the adsorbed water to form hydroxyl radical. Finally, the active species, holes, superoxide anion radical and hydroxyl radical oxidize the Methylene blue and Malachite green dye molecules adsorbed on the active sites of the barium tungstate-graphene oxide system through the  $\pi$ - $\pi$  stacking and electrostatic attraction.



Scheme-1 Plausible Mechanism for photocatalytic activity.

### IV. CONCLUSION

The BaWO<sub>4</sub> and Graphene Oxide were prepared by the simple, low-temperature route. Furthermore, they were characterized by the XRD, FTIR, SEM, EDAX, Raman Spectroscopy and UV-visible Spectrophotometer techniques. The XRD patterns show the prepared samples are of tetragonal-type structure. No impurity phase has been observed in XRD. The SEM studies confirmed the presence of granular-like grains in the samples. The EDAX data confirmed the presence of corresponding elements in the samples. The band gap data obtained on the sample based on absorbance spectra studies are similar to the reported data. It was found that among the samples studied, the as-prepared BaWO<sub>4</sub>-GO composite with H<sub>2</sub>O<sub>2</sub> is more effective in degrading the Methylene blue and Malachite green dye present in the water sample in presence of visible light at the wave length of 657nm and 617 nm at normal room temperature. Hence, BaWO<sub>4</sub> nanoparticles are suggested as a potential candidate to remove organic pollutants present in water by simple photocatalysis at room temperature.

### ACKNOWLEDGEMENTS

Authors thank the UGC, SERO, Hyderabad for providing UGC-FDP Teacher Fellowship to M. Sunitha and UGC, MHRD, New Delhi for providing financial assistance through UGC-MRP No.41-371/2012(SR) to S.Paul Douglas. Authors thank Prof. M. Uma Bala, HOD, Dept. of Inorganic and Analytical Chemistry, Andhra University for UV-DRS studies, IICT Hyderabad for SEM, FT-IR and XRD, Centre for Nanotechnology, AUCE (A), AU for ball milling and JNTUK, Kakinada for Raman spectral studies.

### REFERENCES

- [1] P. Suresh, A.M.Umabala, T.Siva Rao and A. V. PrasadaRao."Visible Light Induced Synergistic Degradation of Rhodamine-B, Methylene Blue And

- Malachite Green By  $\text{Fe}_2(\text{MoO}_4)_3$  And  $\text{MoO}_3$ ". Journal of Applicable Chemistry, vol. 3 (2), pp. 696-701, 2014.
- [2] H.Zheng, Y.Li, H. Liu, X.Yin and Y. Li. Construction of heterostructure materials toward functionality'. Chem. Soc. Rev, vol.40, pp. 4506-4524, 2011.
- [3] K.Liu, K.Nagodawithana, P.C. Searson and C.L. Chien, "Perpendicular giant magnetoresistance of multilayered Co/Cu nanowires". Physical Review B Condensed matter, vol. 51, pp.7381-7384, 1995.
- [4] M. Bognitzki, H. Hou, M. Ishaque, T. Frese, M. Hellwig, C. Schwarte, A. Schaper, J. H.Wendorff, A. Greiner, "Polymer, metal, and hybrid nano- and mesotubes by coating degradable polymer template fibers (TUFT Process)". Adv. Mater, vol 12, pp 637-640, 2000.
- [5] D. J.Milliron, S. M. Hughes, Y.Cui, L.Manna, J. Li, L.-W.Wang and A.P.Alivisatos, "Colloidal nanocrystal heterostructures with linear and branched topology". Nature, vol 430, pp190-195, 2004.
- [6] A. J.Mieszawska, R.Jalilian, G. U. Sumanasekera and F. P. Zamborini, "Synthesis of gold nanorod/single-wall carbon nanotube heterojunctions directly on surfaces". J. Am. Chem. Soc., vol 127, pp 10822-10823, 2005.
- [7] C.Li, Y.Chen, Y.Wang, Z. Iqbal, M. Chhowalla and S. Mitra, "A fullerene-single wall carbon nanotube complex for polymer bulk heterojunction photovoltaic cells". J. Mater. Chem., vol.17, pp 2406-2411, 2007.
- [8] L. J.Lauhon, M. S.Gudiksen, D.Wang, C. M. Lieber, "Epitaxial core-shell and core-multishell nanowire heterostructures". Nature, vol 420, pp 57-61, 2002.
- [9] Q.Wang, G.Wang, B.Xu, J.Jie, X. Han, G. Li, Q. Li and J. G. Hou, "Non-aqueous cathodic electrodeposition of large-scale uniform ZnO nanowire arrays embedded in anodic alumina membrane". Mater. Lett., vol 59, pp 1378-1382, 2005.
- [10] M.Nikl, P.Bohacek, E.Mihokova et al., "Excitonic emission of scheelite tungstates  $\text{AWO}_4$  (A = Pb, Ca, Ba, Sr)". Journal of Luminescence, vol. 87, pp. 1136-1139, 2000.
- [11] A. J. Lee, H. M. Pask, J. A. Piper, H. Zhang, and J. Wang, "An intracavity, frequency-doubled  $\text{BaWO}_4$  Raman laser generating multi-watt continuous-wave, yellow emission". Optics Express, vol. 18, no. 6, pp. 5984-5992, 2010.
- [12] P. Cerny, H. Jelinkova, P.G.Zverev, and T. T. Basiev, "Solid state lasers with Raman frequency conversion". Progress". Quantum Electronics, vol. 28, no. 2, pp. 113-143, 2004.
- [13] T.T.Basiev, V.Osiko, A.M.Prokhorov and E.M.Dianov, "Crystalline and fiber raman lasers" Solid-State Mid-Infrared Laser Sources, vol. 89, pp. 359-408, 2003.
- [14] J. Ninkovica, G. Angloher, C. Bucci et al., " $\text{CaWO}_4$  crystals as scintillators for cryogenic dark matter search, Nuclear Instruments and Methods". Physics Research A, vol. 537, no. 1-2, pp. 339-343, 2005.
- [15] A. Caprez, P. Meyer, P. Mikhail, and J. Hulliger, "New host-lattices for hyperfine optical hole burning: materials of low nuclear spin moment". Materials Research Bulletin, vol. 32, no. 8, pp. 1045-1054, 1997.
- [16] P. Afanasiev, "Molten salt synthesis of barium molybdate and tungstate microcrystals". Materials Letters, vol. 61, no. 23-24, pp. 4622-4626, 2007
- [17] F.J. Manjon, D. Errandonea, N. Garro, J.Pellicer-Porres, P.Rodriguez-Hernandez, S. Radescu, J.Lopez-Solano, A. Mujica and A. Munoz, "Lattice dynamics of scheelite tungstates under high pressure I.  $\text{BaWO}_4$ ". Physical Rev. B. vol. 74, pp. 144111-144117, 2006.
- [18] Kinga Haubner, Jan Morawski, Phillip Olk, Lukas M. Eng, Christoph Ziegler, Barbara Adolphi and Evelin Jaehne "The route to functional graphene oxide". vol. 10, pp. 1002/cphc.200.
- [19] J. Zhang, Z.H.Huang, Y. Xu and F.Kang, "Hydrothermal Synthesis of Graphene / $\text{Bi}_2\text{WO}_6$  Composite with High Adsorptivity and Photoactivity for Azo Dye". J. Am. Ceram. Soc., vol. 96 [5], pp.1562-1569, 2013.
- [20] D.D. Dionysiou, M.T .Suidam, I. Baudin, J.-M.Laîné, "Effect of hydrogen peroxide on the destruction of organic contaminants -Synergism and inhibition in a continuous-mode photocatalytic reactor". Appl. Catal. B: Environ., vol. 50, pp.259-269, 2004.
- [21] K.Rajeshwar, "Photo electrochemistry and environment". J. Appl. Electrochem., vol. 25, pp. 1067-1082, 1995.
- [22] J.M.Herrmann, C.Guillard and P.Pichat, "Heterogeneous photocatalysis: An emerging technology for water treatment". Catal. Today, vol. 17, pp.7-20, 1993.
- [23] Paulchamy et al., "A Simple Approach to Stepwise Synthesis of Graphene Oxide Nanomaterial". J Nanomed Nanotechnol, vol.6, pp.1, 2015.
- [24] Jr W.S .Hummers and R.E. Offeman, "Preparation of graphitic oxide". J Am Chem Soc vol.80, pp.1339-1339, 1958.
- [25] M. J.S. Mohamed and D. K. Bhat, "Novel  $\text{ZnWO}_4$ /RGO nano composite as high performance

- photo catalyst". *AIMS Materials Science*, vol. 4(1) pp. 158-171.
- [26] W.K.Jo and H.-J. Kang, "Titanium dioxide-graphene oxide composites with different ratios supported by Pyrex tube for photocatalysis of toxic aromatic vapors". *Powder Technology* vol.250, pp.115, 2013.
- [27] H. L. Li, Z. L.Wang, S. J. Xu, and J. H. Hao "Improved Performance of Spherical BaWO<sub>4</sub>:Tb<sup>3+</sup> Phosphors for Field-Emission Displays". *Journal of The Electrochemical Society*, vol. 156, pp. 5J112-J116, 2009.
- [28] P. Parhi, T.N. Karthik and V. Manivannan "Synthesis and characterization of metal tungstates by novel solid-state metathetic approach". *Journal of Alloys and Compounds* vol.1 465, pp.380–386, 2008.
- [29] P.H. Bottlebergs, H. Everts and G.H.J. Broers, "Optical nonlinearities of conjugated molecules. Stilbene derivatives and highly polar aromatic compounds". *Mater. Res. Bull.*vol. 11,pp. 263, 1976.
- [30] A.M.Golub, V.I.Maksin, A.A.Kapshuk and S.A. Kirillov, "inorganic chemistry of the transition metals". *Russ. J. Inorg. Chem.*,vol. 2 ,pp. 1310,1976.
- [31] S. Vidya, S.Solomon, J. K. Thomas, "Synthesis, Characterization, and Low Temperature Sintering of Nanostructured BaWO<sub>4</sub> for Optical and LTCC Applications". *Hindawi Publishing Corporation Advances in Condensed Matter Physics* Vol. 2013, pp.1-11, 2013.
- [32] K.Kim and Y.-D.Huh Bull. "Facile Synthesis of BaWO<sub>4</sub> Sub-Micron Sized Octahedron via a Microemulsion Method". *korean Chem. Soc.*, Vol. 33, pp. 10 3489, 2012.
- [33] M. M. J. Sadiq and A. Samson Nesaraj "Soft chemical synthesis and characterization of BaWO<sub>4</sub> nanoparticles for photocatalytic removal of Rhodamine B present in water sample". *J Nano struct Chem*, Vol. 5, pp. 45–54, 2015.
- [34] M. Zhu, D. Meng , C.Wang ,J. Di and G. Diao, "Degradation of methylene blue with H<sub>2</sub>O<sub>2</sub> over a cupric oxide nanosheet catalyst". *Chinese Journal of Catalysis* vol. 34, pp. 2125–2129, 2013.
- [35] X. Hu, X.Meng and Z. Zhang. "Synthesis and Characterization of Graphene Oxide-Modified Bi<sub>2</sub>WO<sub>6</sub> and Its Use as Photocatalyst". *International Journal of Photoenergy* vol. 10, pp. 1155, 2016.
- [36] X. Meng and Z. Zhan, "Synthesis, analysis, and testing of BiOBr-Bi<sub>2</sub>WO<sub>6</sub> photo catalytic heterojunction semiconductors". *Journal of Photo energy* vol. 10, pp.1155, 2015.